PEP-II/AP Note 4-93
ESG Tech Note-232

DYNAMICAL BETA FUNCTION AND BEAM-BEAM TUNE SHIFT FOR PEP-II

Miguel A. Furman

Center for Beam Physics
Accelerator and Fusion Research Division
Lawrence Berkeley Laboratory, MS 71-H
Berkeley, CA 94720

January 3rd, 1994

ABSTRACT

We present the calculation of the beam-beam tune shift and dynamical beta function for PEP-II as a function of the fractional tune and the beam separation at the parasitic collision (PC) points. We do the calculation both for "typical" and for "pacman" bunches taking into account all the PCs. We show that the approximation in which one keeps only the effects of the first PCs on either side of the interaction point (IP) is a good one except very close to the stopbands. The results presented here provide some basic constraints in the choice of the working point. This note corrects, updates and extends previous work contained in Refs. [1] and [2].

1. Introduction.

If the beam-beam interaction is relatively weak, as is the case for most colliders, one can assess, in linear approximation, some of its most basic constraints on the luminosity performance of a collider. In this approximation one represents the beam-beam collision as a thin-lens kick located at the IP that has the property of being focusing in both planes. This linear analysis of the beam-beam interaction has the value of exhibiting constraints that are absolutely necessary, although far from sufficient, for acceptable luminosity performance; however, it is probably irrelevant to the luminosity lifetime problem. Obviously this approximation is insensitive to all synchro-betatron resonances, and to all betatron resonances except those near the integer and half-integer tunes. Earlier discussions on the dynamical beta function for PEP-II were presented in Refs. [1] and [2]. This note corrects some mistakes in the earlier work, updates it to current PEP-II parameters, and extends the discussion by including the effects of all the PCs and for pacman bunches.

There are three well-known consequences that follow from the linear approximation: (1) Stopbands near integer and half-integer tunes appear. (2) The tune shift produced by the beam-beam collision is significantly different from the beam-beam parameter near the edges of the

stopband. (3) The beta function at the IP is different from its nominally-specified value (this is the so-called "dynamical beta function" effect). In this note we compute the edges of the stopbands, the beam-beam tune shifts and the dynamical beta functions at the IP for the specific case of PEP-II, as a function of tune. We take into account all PCs, and we also carry out the calculation for pacman bunches, not just typical bunches.

We conclude that: (1) It is advantageous to choose a working point just above the integer or the half-integer because the dynamical beta function is smaller than the nominal and the tune shift is smaller than the beam-beam parameter. (2) The vertical beam-beam tune shifts and dynamical beta functions, especially those of the low-energy beam (LEB), are much more sensitive than the horizontal ones to the beam separation at the PC: for small enough separation, both the tune shift and the dynamical beta function become large, undoing the favorable effect of the choice of the working point just mentioned. (3) The approximation in which the "outer" PCs are neglected and only the PCs closest to the IP are taken into account is a good one. (4) The approximation in which the beam-beam tune shifts are computed by simply adding linearly the beam-beam parameters at the IP and all PCs (i.e., neglecting the intervening phases advances) is also a legitimate one for most values of the fractional tune. (5) As a corollary of the previous two conclusions, the effects for the pacman bunches can be estimated by simply adding the contributions to the beam-beam parameters from the subset of collisions experienced by these bunches. (6) If the working point is chosen to be $(\nu_x, \nu_y)=(0.64, 0.57)$ for both beams, the vertical "pacman tune spread" of the LEB is ~0.006 and that of the HEB is ~0.004, while their horizontal counterparts are much smaller; these spreads can be reduced, if necessary, by choosing a working point with larger fractional tune.

2. Calculation in linear theory.

Each beam-beam collision, whether it is head-on or long-range, is characterized in lowest order by a beam-beam parameter, which measures the strength of the collision experienced by the particle at the center of the bunch. In the small-amplitude approximation, the n-th collision experienced by the particle is described by the linear kick

$$\Delta x' = -k_n x \tag{1}$$

where x is the displacement from the nominal orbit. The kick strength k_n is related to the beam-beam parameter ξ_n by the definition

$$k_n \equiv \frac{4\pi\xi_n}{\beta_n} \tag{2}$$

where β_n is the lattice beta-function at the collision point (k_n is also equal to the inverse of the focal length of the kick). The sign convention implied by Eq. (1) is that, for focusing kicks, $k_n > 0$ and hence $\xi_n > 0$.

We assume that the lattice is linear and that there is no x-y coupling; therefore we can treat the horizontal and vertical phase spaces separately in the two rings. We label the parasitic collisions $n = 1,...,4$ or $n = -4,...,-1$ as shown in Fig. 1, and we call $n = 0$ the main collision at the IP. With

this labeling convention, the one-turn map for a particle corresponding to a surface of section immediately before the IP is given by

$$M'(0) = M(0,-1)K(-1)\cdots K(-4)M(-4,4)K(4)\cdots K(1)M(1,0)K(0) \tag{3}$$

where $K(n)$ is the beam-beam kick at collision n

$$\begin{pmatrix} x \\ x' \end{pmatrix}_{after} = K(n)\begin{pmatrix} x \\ x' \end{pmatrix}_{before} \quad , \quad K(n) \equiv \begin{pmatrix} 1 & 0 \\ -k_n & 1 \end{pmatrix} \tag{4}$$

and $M(n,m)$ is the linear transport matrix [3] from point m to point n,

$$\begin{pmatrix} x \\ x' \end{pmatrix}_n = M(n,m)\begin{pmatrix} x \\ x' \end{pmatrix}_m \tag{5}$$

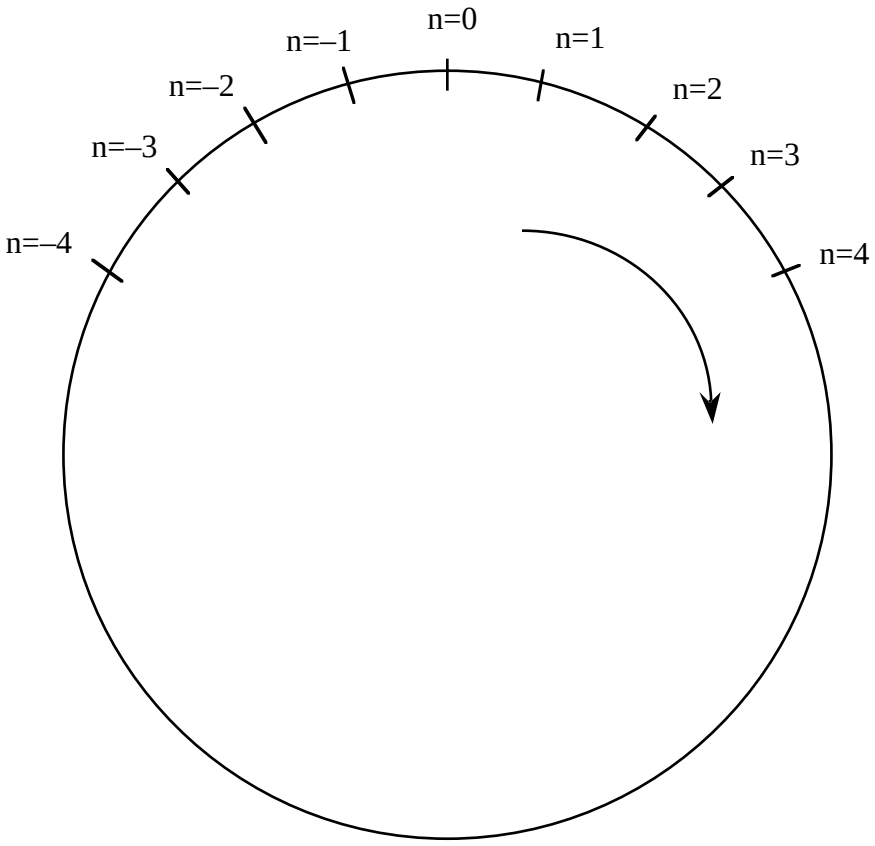

Fig. 1 Sketch of the beam-beam collisions around the ring. n=0 represents the main collision at the IP. The others collisions are parasitic. The beam moves in the direction indicated by the arrow.

given by

$$M(n,m) \equiv \begin{pmatrix} \sqrt{\frac{\beta_n}{\beta_m}}\left(C_{nm} + \alpha_m S_{nm}\right) & \sqrt{\beta_n \beta_m}\, S_{nm} \\ -\frac{\left(1+\alpha_n\alpha_m\right)S_{nm} + \left(\alpha_n - \alpha_m\right)C_{nm}}{\sqrt{\beta_n\beta_m}} & \sqrt{\frac{\beta_m}{\beta_n}}\left(C_{nm} - \alpha_n S_{nm}\right) \end{pmatrix} \tag{6}$$

Here the α's and the β's are the usual (unperturbed) lattice functions at points m and n, S_{nm} and C_{nm} are given by $S_{nm} \equiv \sin(\phi_n - \phi_m)$ and $C_{nm} \equiv \cos(\phi_n - \phi_m)$ where $\phi_n - \phi_m$ is the phase advance from point m to point n, which is determined by the optics of the interaction region (IR). The phase advance of the long arc from n=4 to n=–4 is determined by these phases and by the overall tune of the ring.

Once the right-hand side of Eq. (3) is computed, the beam-beam tune shift and the dynamical beta function at the IP can be extracted from the one-turn map $M'(0)$, defined by

$$M'(0) \equiv \begin{pmatrix} C' + \alpha' S' & \beta' S' \\ -\gamma' S' & C' - \alpha' S' \end{pmatrix} \tag{7}$$

where the primes denote perturbed quantities. In particular, β' is the dynamical beta function. The beam-beam tune shift $\Delta\nu$ is related to C' and S' via $C' \equiv \cos(2\pi\nu')$ and $S' \equiv \sin(2\pi\nu')$ where $\nu' \equiv \nu + \Delta\nu$ and ν is the unperturbed, or "bare lattice," tune. The next step in the numerical calculation is to extract $\Delta\nu$ from the relation

$$\mathrm{tr}M'(0) = 2\cos\left(2\pi(\nu + \Delta\nu)\right) \tag{8}$$

and the final step is to extract β' by equating the (1,2) matrix elements of Eqs. (3) and (7).

In the next Section we present the numerical results for PEP-II obtained from this procedure. However, it is instructive to look at the expressions in lowest-order perturbation theory. In the Appendix we show how the analytical calculation can be considerably simplified by going to the normalized coordinate basis. If all the PCs are ignored, the expressions for the tune shift and the dynamical beta function are given, to first order in ξ_0, by the well-known results [3]

$$\Delta\nu = \xi_0 + \cdots \tag{9}$$

$$\frac{\beta'}{\beta} = 1 - 2\pi\xi_0 \cot(2\pi\nu) + \cdots \tag{10}$$

and the stopband occurs for

$$\frac{p}{2} - \delta\nu < \nu < \frac{p}{2} \tag{11}$$

where p is any integer, and where the stopband width $\delta\nu$ is given by

$$\delta\nu = 2\xi_0 + \cdots \tag{12}$$

($\Delta\nu$ and β'/β are periodic functions of ν with a period of one-half a unit). However, the PCs modify these results significantly: the expressions for the tune shift and dynamical beta function,[1] to first order in *any* of the ξ's, are given by [3]

$$\Delta\nu = \sum_{n=-4}^{4} \xi_n + \cdots \tag{13}$$

$$\frac{\beta'}{\beta} = 1 - \frac{2\pi}{\sin(2\pi\nu)} \sum_{n=-4}^{4} \xi_n \cos\left(2\Delta\phi_n - 2\pi\nu\right) + \cdots \tag{14}$$

If the stopband is defined by the interval $\nu_- \le \nu \le \nu_+$, and if the optics of the IR is symmetrical about the IP (as is the case in PEP-II), then the edges $\nu_\pm$ are given, in this approximation, by (see Appendix)

$$\begin{aligned} \nu_+ &= \frac{p}{2} - 4\sum_{n\ge 1} \xi_n \sin^2 \phi_n + \cdots \\ \nu_- &= \frac{p}{2} - 2\xi_0 - 4\sum_{n\ge 1} \xi_n \cos^2 \phi_n + \cdots \end{aligned} \tag{15}$$

and the stopband width is

$$\delta\nu \equiv \nu_+ - \nu_- = 2\xi_0 + 4\sum_{n\ge 1} \xi_n \cos 2\phi_n + \cdots \tag{16}$$

3. Applications to PEP-II.

3.1 Input parameters.

The beam-beam parameters for a particle at the bunch center are computed from the usual formulas. Assuming that the bunch distribution is gaussian in the transverse dimensions, the vertical beam-beam parameter for the head-on collision at the IP for a positron is given by

$$\xi_{0y+} = \frac{r_0 N_- \beta_{y+}}{2\pi\gamma_+ \sigma_{0y-}(\sigma_{0x-} + \sigma_{0y-})} \tag{17}$$

where r_0 is the classical electron radius, N_- is the number of electrons in the opposing bunch, the σ's are the rms electron beam sizes, and γ_+ is the usual relativistic factor for the positrons. The

---

[1] Eq. (4.49) in Ref. [3] has two sign errors which, unfortunately, have propagated through some of the literature. The equations leading up to Eq. (4.49) are correct, but there is an error in the trigonometry at the very last step of the derivation. Our Eq. (14) is the correct result for discrete kicks.

corresponding expressions for the other three parameters are obtained from the above by the exchanges $x \leftrightarrow y$ and/or $+ \leftrightarrow -$. The subscript "0" for ξ and the σ's means "nominal quantities," i.e., in the absence of the dynamical effects from the beam-beam interaction (in this note we do not take into account any such dynamical effects). For horizontal beam separation the long-range beam-beam parameters at the PCs for the positrons are given by

$$\xi_{0x+} = -\frac{r_0 N_- \beta_{x+}}{2\pi\gamma_+ d^2}, \qquad \xi_{0y+} = +\frac{r_0 N_- \beta_{y+}}{2\pi\gamma_+ d^2} \tag{18}$$

with similar expressions for the electrons, obtained from these by exchanging $+ \leftrightarrow -$. These formulas are valid when the beam centers are separated by a distance d that is much larger than the rms beam size at the PC. This last condition is well-satisfied by the PEP-II IR design (see Table 2 below).

Numerical values for all necessary quantities for the high-energy beam (HEB) and the low-energy beam (LEB) are listed in Tables 1 and 2 (some of these quantities are not used in the present calculation). The ϕ's that appear in Eqs. (6) and (14–16) are the phases of the collision points relative to the IP and are related to the ν's by $\phi = 2\pi\nu$. The optics is symmetrical about the IP, so we only list the lattice functions for $n \geq 0$.

Table 1. Main PEP-II IR parameters.

n	d [mm]	β_x [m]	β_y [m]	α_x	α_y	ν_x	ν_y
			LEB (e^+)				
0	0.0	0.375	0.015	0.0	0.0	0.000	0.000
1	3.498	1.433	26.460	–1.679	–41.98	0.165	0.246
2	17.651	4.607	105.63	–3.362	–83.77	0.204	0.248
3	39.114	16.202	133.70	–11.79	–27.96	0.215	0.249
4	71.879	57.171	69.294	–40.76	+34.98	0.218	0.250
			HEB (e^-)				
0	0.0	0.500	0.020	0.0	0.0	0.000	0.000
1	3.498	1.293	19.853	–1.260	–31.49	0.143	0.245
2	17.651	3.673	79.340	–2.519	–62.96	0.190	0.247
3	39.114	9.162	148.29	–5.322	–64.50	0.207	0.248
4	71.879	20.917	189.97	–10.94	–39.35	0.214	0.249

Table 2. Other PEP-II IR parameters.

n	s [m]	η_x [m]	σ_{0x} [mm]	σ_{0y} [mm]	d/σ_{0x}	ξ_{0x}	ξ_{0y}
			LEB (e^+)				
0	0.0	0.000	0.151573	0.006063	0.0	+0.03	0.03
1	0.630	0.002	0.296	0.255	11.8	–0.000224	0.004134
2	1.260	0.024	0.531	0.509	33.2	–0.000028	0.000648
3	1.889	0.061	0.996	0.572	39.3	–0.000020	0.000167
4	2.519	0.138	1.872	0.412	38.4	–0.000021	0.000026
			HEB (e^-)				
0	0.0	0.000	0.151573	0.006063	0.0	+0.03	0.03
1	0.630	0.001	0.244	0.191	14.3	–0.000152	0.002326
2	1.260	0.009	0.411	0.382	43.0	–0.000017	0.000365
3	1.889	0.017	0.649	0.522	60.3	–0.000009	0.000139
4	2.519	0.028	0.980	0.591	73.3	–0.000006	0.000053

3.2 Tune shifts and dynamical beta functions for typical bunches.

A “typical bunch” is one that is far away (at least four bunch spaces) from either end of the bunch train, and therefore experiences all PCs, in addition to the main collision at the IP [5]. Fig. 2 shows the tune shift for a typical bunch plotted vs. the bare lattice tune (the figure repeats with a periodicity of one-half a unit of tune). One sees that the vertical tune shifts, particularly that of the LEB, are clearly higher than the nominal beam-beam parameter value of 0.03. The horizontal tune shift becomes small just above the integer (or half-integer), and the vertical tune shift becomes small just *below* the half-integer (or integer). However, these values of the tune should be avoided because the closed orbit distortion becomes large [5].

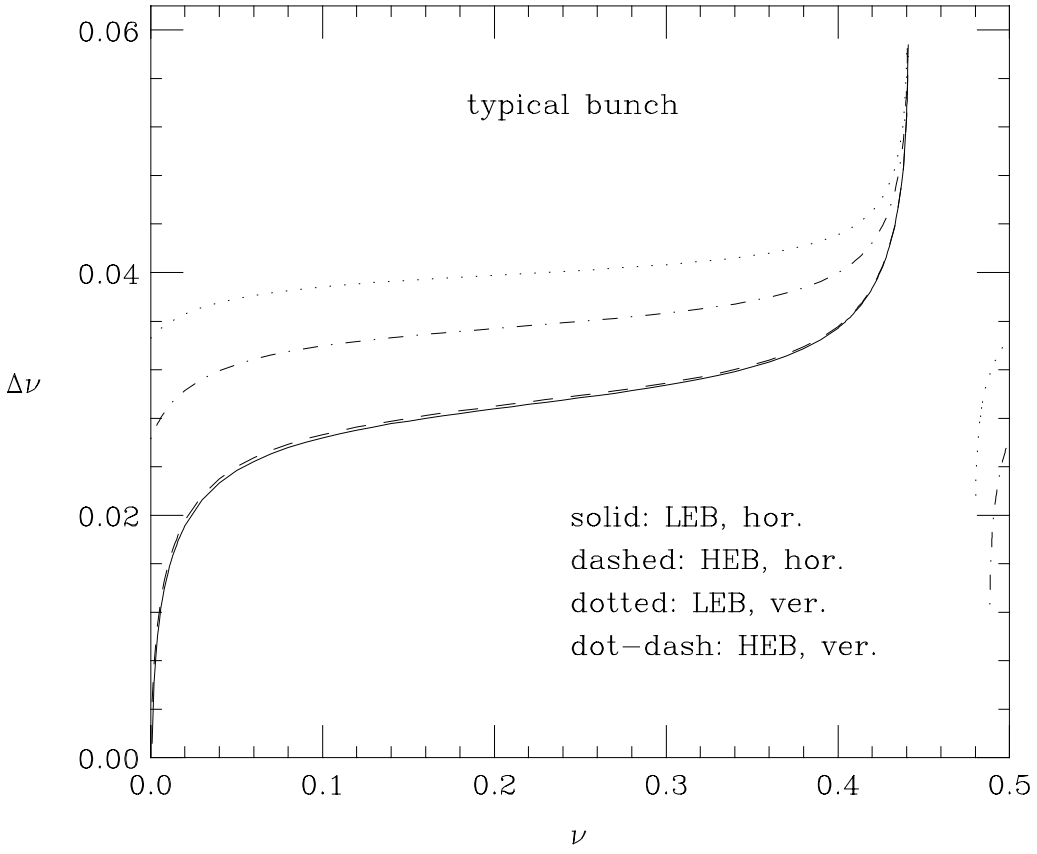

Fig. 2 The horizontal and vertical beam-beam tune shift for a typical bunch as a function of the corresponding tune for nominal PEP-II parameters. The figure is periodic in ν with a period of 0.5.

The location and width of the horizontal stopbands are in good agreement with the lowest-order estimate in the absence of the PCs, Eqs. (11–12). The vertical stopbands, however, are downshifted in tune by ~0.02 for the LEB and by ~0.01 for the HEB. Table 3 shows the numerical results obtained for the stopbands, corresponding to Fig. 2, along with the estimates obtained from Eqs. (15–16). The downshift of the vertical stopbands is accounted for by the fact that the vertical ξ's are >0 (cf. Eqs. (17–18)). Only when the PCs are taken into account does one find good agreement with the exact numerical calculation. It is interesting to note also that another effect of the PCs is to *narrow* the stopband that would be produced by the IP alone. This is particularly true for the vertical stopbands, for which this narrowing is easily explained by noting that the ϕ's are all very close to $\pi/2$, hence $\cos 2\phi_n \approx -1$ in Eq. (16).

Table 3. Exact and approximate stopband edges and widths. [a)]

	LEB (e^+)			HEB (e^-)		
	Eq. (11/12)	Eq. (15/16)	Numerical	Eq. (11/12)	Eq. (15/16)	Numerical
ν_{x-} [b)]	0.4400	0.4403	0.4408	0.4400	0.4402	0.4408
ν_{x+} [b)]	0.5000	0.5009	0.5001	0.5000	0.5005	0.5001
ν_{y-} [b)]	0.4400	0.4400	0.4401	0.4400	0.4400	0.4404
ν_{y+} [b)]	0.5000	0.4801	0.4802	0.5000	0.4885	0.4885
$\delta\nu_x$	0.0600	0.0607	0.0592	0.0600	0.0602	0.0592
$\delta\nu_y$	0.0600	0.0401	0.0402	0.0600	0.0485	0.0485

[a)] The tune is here restricted to its basic period, namely $0 < \nu < 1/2$.
[b)] The subscripts + and – refer to the upper and lower edges of the stopband, respectively, and not to the beam.

The remarkable (but approximate) coincidence of the four lower edges ν_- of the stopbands seems to be due to an accidental conspiracy between the phases and the beam-beam parameters of the PCs, Eq. (15).

Fig. 3 shows the dynamical beta functions, normalized to their nominal values, plotted vs. tune. One can see that the dynamical beta functions are smaller than their nominal counterparts for tunes $\lesssim 0.25$. This is qualitatively explained by the cotangent-term in Eq. (10). The difference between the four curves in Fig. 3 is due to the PCs: if the PCs were ignored, the four curves would overlap.

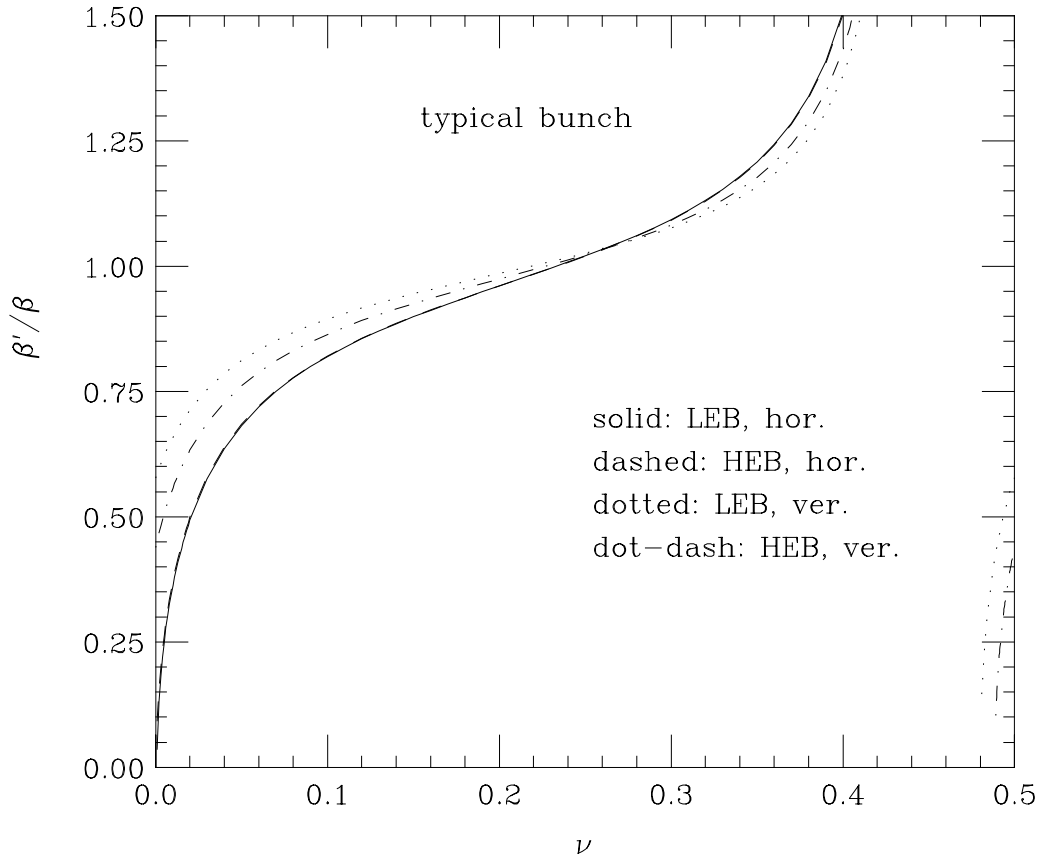

Fig. 3 The horizontal and vertical normalized dynamical beta function for a typical bunch as a function of the corresponding tune for nominal PEP-II parameters. The figure is periodic in ν with a period of 0.5.

3.3 Tune shifts and dynamical beta functions for pacman bunches.

Fig. 4 shows the beam-beam tune shifts for the first pacman bunch, i.e., the bunch at the head of the train. This bunch experiences the main collision at the IP plus the PCs at one side of the IP only. By symmetry, the results for the last bunch at the tail of the beam are identical to those for the head bunch. The beam-beam tune shifts for the other pacman bunches are in between those for the first pacman bunch and those for a typical bunch, shown in Fig. 2. By comparing the two figures, one can see that there is almost no difference for the horizontal tune shifts, since for these the PCs are quite negligible. For the vertical tune shifts, the effect of the PCs for the first pacman

bunch are, roughly speaking, about half as strong as for a typical bunch, hence the values for the tune shifts are about half way in between the horizontal values and those for a typical bunch.

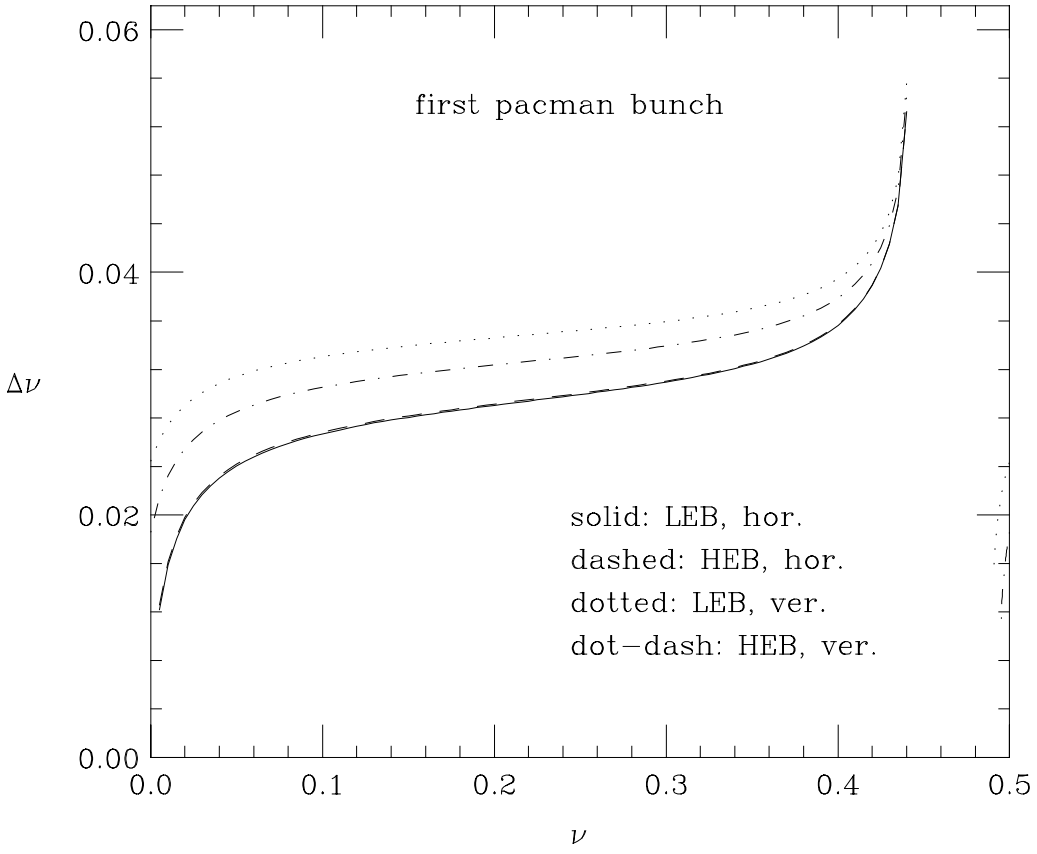

Fig. 4 The horizontal and vertical beam-beam tune shift for the first pacman bunch, as a function of the corresponding tune for nominal PEP-II parameters. The figure is periodic in ν with a period of 0.5.

By the same reasoning mentioned above, the horizontal normalized dynamical beta functions for the head bunch (not shown) are almost exactly the same as those for a typical bunch, while the vertical normalized dynamical beta functions are somewhere in between the horizontal values and those for a typical bunch.

Once a working point is chosen, we can estimate the "pacman tune spread," i.e., the tune spread due to the ion-clearing gap, by forming the difference, in absolute value, between the tune shift of a typical bunch and that of the first pacman bunch. For example, if we set $(\nu_x, \nu_y)=(0.64, 0.57)$ for both beams, which is a choice that has been made in many beam-beam simulation studies [4], we obtain the results in Table 4.

Table 4. Pacman tune spreads for the working point (0.64, 0.57).

	LEB (e^+)	HEB (e^-)
horizontal	0.0003	0.0002
vertical	0.006	0.004

In accordance with Eq. (13), a simple-minded estimate of the pacman tune spread would be

$$\text{pacman tune spread} \approx \sum_{n\geq 1} \xi_n \tag{19}$$

which yields ~0.005 for the vertical pacman tune spread of the LEB. The difference between this estimate and the actual value of 0.006 in Table 4 is due to the tune dependence of the tune shift, which does not enter in Eq. (19). The value of 0.006 represents 20% of the nominal beam-beam parameter value of 0.03, which may be deemed a sizable fraction. It should be noted, however, that the pacman tune spread becomes smaller as the tune increases. Therefore, if further studies show that 0.006 is too large a spread, it can be reduced by choosing a vertical working point higher than 0.57.

3.4 Results when only the first PCs are considered.

From Table 2 one can see that the first PC is significantly stronger than the others. In many simulation studies [4], all PCs beyond the first have been neglected for calculational simplicity. Fig. 5 shows a comparison of the calculation of the vertical tune shift of a typical LEB bunch in three cases: IP only (all PCs are neglected), IP plus first PCs, and IP plus all PCs. One can see that there is relatively little difference between the last two cases, but there is a significant difference between the first and second cases. Of the four tune shifts (horizontal and vertical for both beams) we only show the vertical tune shift of the LEB because it is for this case that the difference between the results in the three approximations just mentioned is largest.

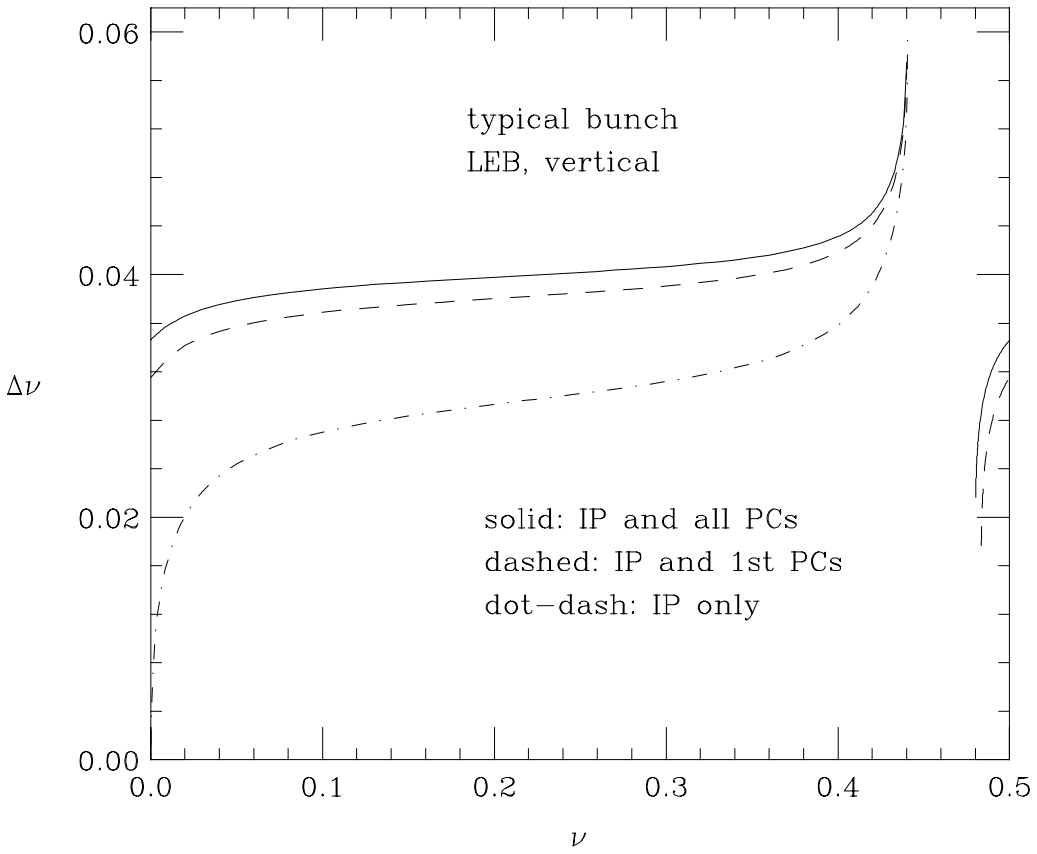

Fig. 5 The vertical beam-beam tune shift for a typical LEB bunch, as a function of the tune, computed in three approximations. The figure is periodic in ν with a period of 0.5.

Figure 6 shows the beam-beam tune shifts of a typical bunch plotted vs. the normalized beam separation at the first PC. In this calculation all PCs beyond the first have been neglected, the beam separation *d* is taken as a free parameter, and the fractional tunes are fixed at (ν_x, ν_y)=(0.64, 0.57) for both beams. All other parameters are fixed at their nominal PEP-II values [4]. One can see that the vertical tune shift, particularly that of the LEB, becomes large quickly as the beam separation decreases from its nominal value.

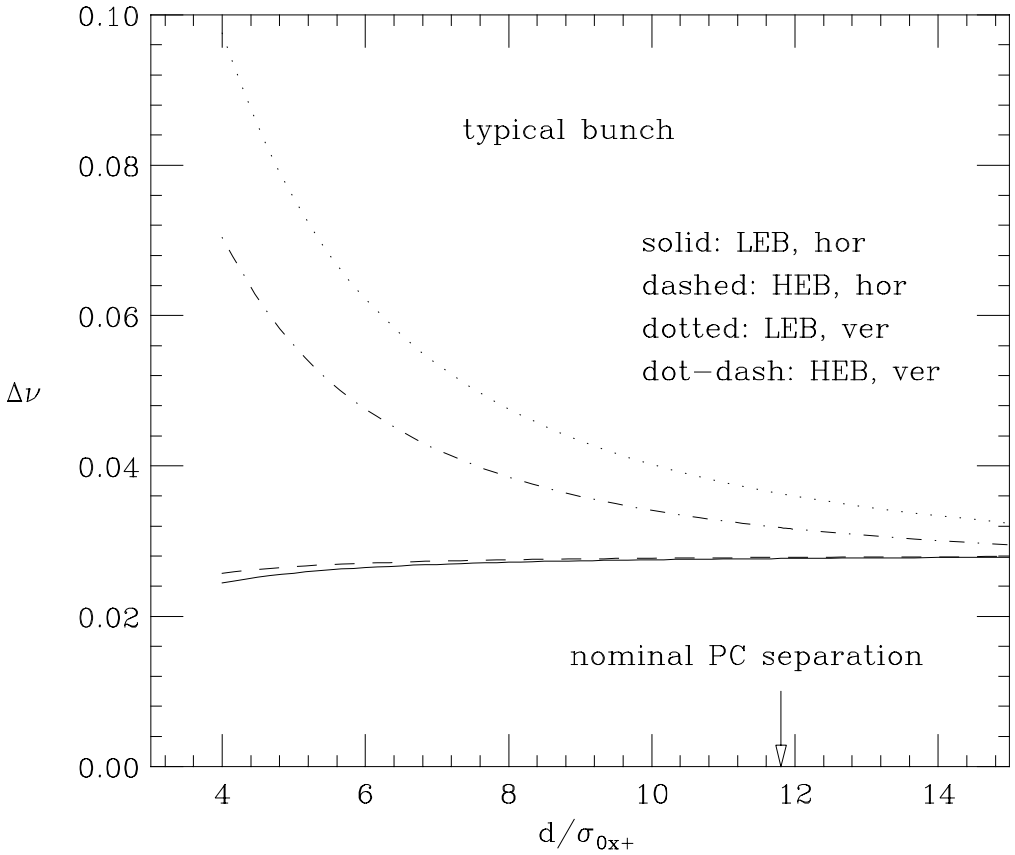

Fig. 6 The beam-beam tune shifts of a typical bunch as a function of the beam separation at the first PC. The beam separation is normalized to the local nominal horizontal beam size of the LEB. The fractional tunes are fixed at (ν_x, ν_y)=(0.64, 0.57) for both beams, and all other parameters have their nominal PEP-II values. The arrow indicates the nominal separation, as specified in the CDR [4].

Figure 7 shows the "total beam-beam parameters" of a typical bunch, defined as

$$\xi_{0,tot} \equiv \xi_0 + 2\xi_1 \tag{20}$$

plotted vs. the normalized beam separation at the first PC. The calculation is carried out under the same conditions as in Fig. 6. By comparing Figs. 6 and 7 one can see that $\xi_{0,tot}$ is a good approximation to $\Delta\nu$, as expected from Eq. (13). However, this approximation is not a good one when the tunes are close to the edges of the stopband.

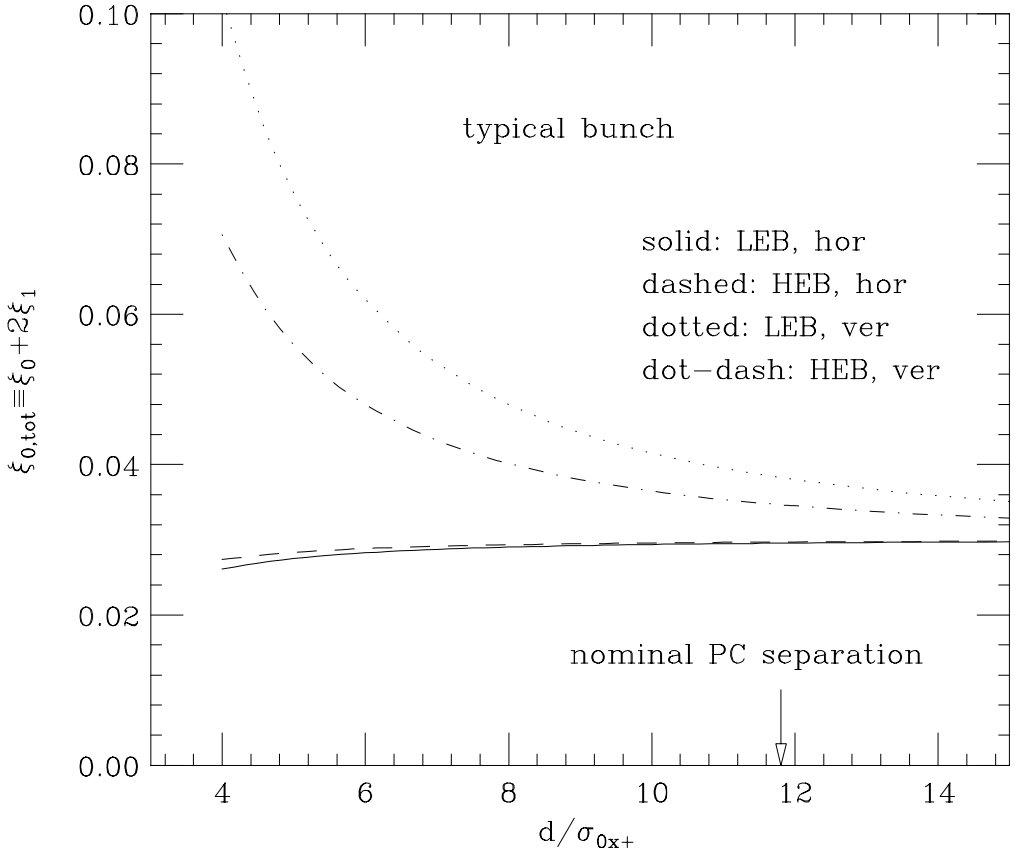

Fig. 7 The total beam-beam parameters of a typical bunch as a function of the beam separation at the first PC. The calculation is carried out under the same conditions as in Fig. 6.

Figure 8 shows the square roots of the normalized dynamical beta functions of a typical bunch plotted vs. the normalized beam separation at the first PC. The calculation is carried out under the same conditions as in Figs. 6 or 7. For the nominal separation, all four dynamical beta functions are smaller than their nominal counterparts as a result of the fact that the tunes are just above the half-integer. However, one sees that, as the beam separation becomes smaller and smaller, the vertical dynamical beta functions grow until they exceed their nominal counterparts. This is due to the fact that the vertical beam-beam parameters increase as d decreases (cf. Eq. (18)); thus when d becomes small enough, the (dynamical) tunes are shifted to sufficiently high values that the dynamical reduction of the beta function is lost.

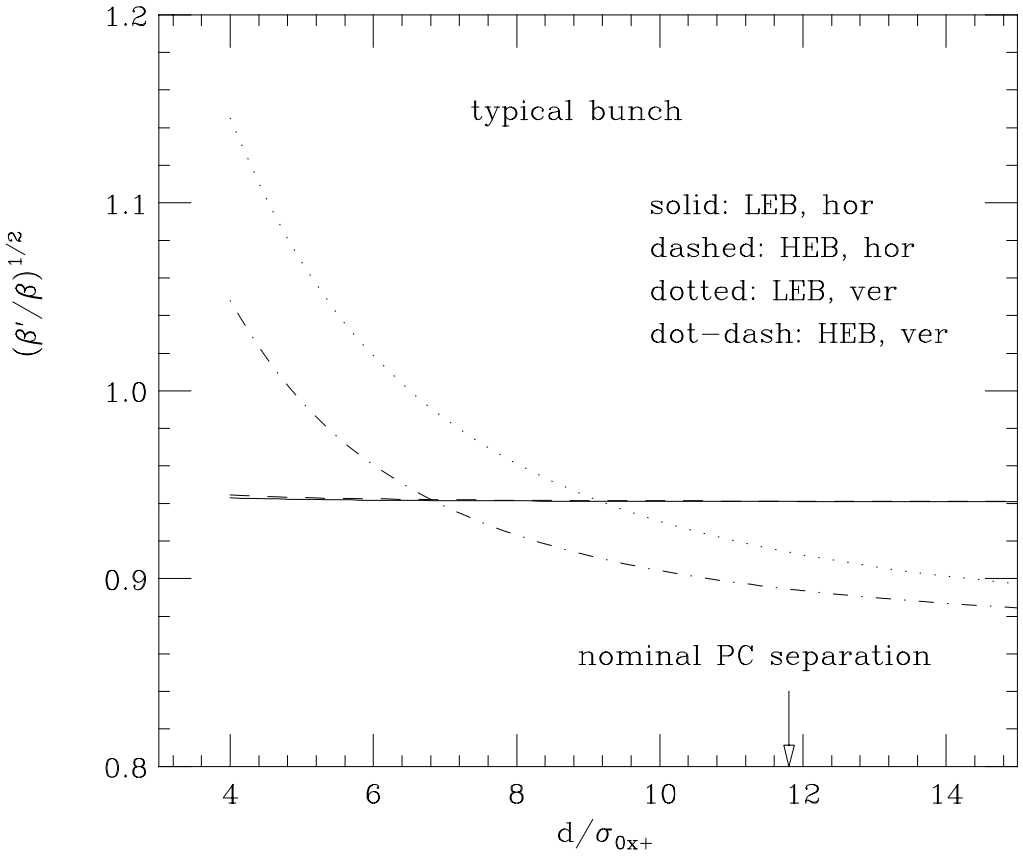

Fig. 8 The square roots of the normalized dynamical beta functions of a typical bunch as a function of the beam separation at the first PC. The calculation is carried out under the same conditions as in Fig. 6.

4. Conclusions.

We have presented the exact numerical calculation of the tune shift and the dynamical beta function for PEP-II in linear theory. In this approximation a stopband appears just below integer and half-integer tunes. We have presented first-order analytic expressions for the results, including the stopband edges and width. We have considered the effects from all the PCs and we have carried out the calculation for typical and for pacman bunches.

Our results imply constraints on the choice of the working point that are necessary (but far from sufficient) for reliable luminosity performance. For a given specification of the beam-beam parameter, the dynamical beta function is smaller than the nominal and the beam-beam tune shift is smaller than the beam-beam parameter when the tune is slightly above the integer or the half integer. This, combined with the constraints [5] from the sensitivity to closed-orbit distortions (which become large near the integer tune) suggest choosing a working point just above the half-integer. If the working point is chosen to be $(\nu_x, \nu_y)=(0.64, 0.57)$ for both beams, the vertical pacman tune spread of the LEB is ~0.006 and that of the HEB is ~0.004, while their horizontal counterparts are much smaller. Should further work show that these values are too large, they can be reduced by choosing a larger fractional tune.

We have also presented the tune shift and the dynamical beta function as a function of the beam separation d at the first PC for a fixed working point. The vertical quantities are quite sensitive to d, a result which correlates well with the beam blowup observed in multiparticle simulations [4].

5. References.

1. J. L. Tennyson, “Tune Considerations for APIARY 6.3D,” ABC-28, August 1991.

2. V. Ziemann, “Dynamic-Beta Model and Non-Linear Tune Shifts for Parasitic Crossings,” ABC-58, January 29, 1991.

3. E. D. Courant and H. S. Snyder, “Theory of the Alternating Gradient Synchrotron,” Ann. Phys. **3**, 1 (1958).

4. “PEP-II: An Asymmetric B Factory – Conceptual Design Report,” June 1993, LBL-PUB-5379/SLAC-418/CALT-68-1869/UCRL-ID-114055/UC-IIRPA-93-01.

5. M. A. Furman, “Closed-Orbit Distortions for “Typical” and “Pacman” Bunches Induced by the Parasitic Collisions,” PEP-II/AP Note 22-93/CBP Tech Note-022, July 21, 1993.

Appendix.

A.1 Calculation in the normalized basis.

The analytic calculation in perturbation theory is considerably simplified by going to normalized coordinates (q, p) defined by the local symplectic transformation

$$\begin{pmatrix} q \\ p \end{pmatrix} = U(n)\begin{pmatrix} x \\ x' \end{pmatrix}, \qquad U(n) \equiv \frac{1}{\sqrt{\beta_n}}\begin{pmatrix} 1 & 0 \\ \alpha_n & \beta_n \end{pmatrix} \tag{A1}$$

In this local basis, the kick defined by Eq. (4) takes the form

$$\begin{pmatrix} q \\ p \end{pmatrix}_{after} = \tilde{K}(n)\begin{pmatrix} q \\ p \end{pmatrix}_{before} \tag{A2}$$

where the normalized kick matrix $\tilde{K}(n)$ is

$$\tilde{K}(n) \equiv U(n)K(n)U(n)^{-1} = \begin{pmatrix} 1 & 0 \\ -k_n\beta_n & 1 \end{pmatrix} = \begin{pmatrix} 1 & 0 \\ -4\pi\xi_n & 1 \end{pmatrix} \tag{A3}$$

Similarly, the linear transport from point m to point n is described by

$$\begin{pmatrix} q \\ p \end{pmatrix}_n = \tilde{M}(n,m)\begin{pmatrix} q \\ p \end{pmatrix}_m \tag{A4}$$

where the normalized transport matrix $\tilde{M}(n,m)$ is given by

$$\tilde{M}(n,m) \equiv U(n)M(n,m)U(m)^{-1} = \begin{pmatrix} C_{nm} & S_{nm} \\ -S_{nm} & C_{nm} \end{pmatrix} \tag{A5}$$

which is obviously of much simpler form than in the conventional basis, Eq. (6). Thus the fundamental equation for the map, Eq. (3), is written, in normalized coordinates,

$$\begin{aligned} M'(0) &\equiv \begin{pmatrix} C' + \alpha' S' & \beta' S' \\ -\gamma' S' & C' - \alpha' S' \end{pmatrix} \\ &= U(0)^{-1}\tilde{M}(0,-1)U(-1)U(-1)^{-1}\tilde{K}(-1)U(-1)\cdots U(0)^{-1}\tilde{K}(0)U(0) \\ &= U(0)^{-1}\left[\tilde{M}(0,-1)\tilde{K}(-1)\tilde{M}(-1,-2)\cdots\tilde{M}(1,0)\tilde{K}(0)\right]U(0) \end{aligned} \tag{A6}$$

It should be noted that all the U's have canceled out except those at the IP. Therefore the apparent explicit dependence of the tune shift and the dynamical beta function on the α's and β's, contained in the M's in Eq. (3), is an artifact of the conventional representation. Only the phases of the collision points (contained in the $\tilde{M}$'s), the lattice functions of the observation point (contained in $U(0)$) and the ξ's (contained in the $\tilde{K}$'s) are relevant. Of course these phases, as well as the ξ's, depend implicitly on the lattice functions at the collision points.

A.2 Result in closed form for a single kick at the IP.

If one neglects all the PCs, then the problem can be solved in an almost trivial manner. In this case the one-turn map corresponding to a surface of section immediately before the IP is

$$M'(0) = \begin{pmatrix} C+\alpha S & \beta S \\ -\gamma S & C-\alpha S \end{pmatrix} \begin{pmatrix} 1 & 0 \\ -4\pi\xi_0/\beta & 1 \end{pmatrix} \tag{A7}$$

from which one readily finds the equations for $\Delta\nu$ and β',

$$\cos(2\pi(\nu+\Delta\nu)) = \cos(2\pi\nu) - 2\pi\xi_0 \sin(2\pi\nu) \tag{A8}$$

and

$$\frac{\beta'}{\beta} = \frac{\sin(2\pi\nu)}{\sin(2\pi(\nu+\Delta\nu))} = \frac{1}{\sqrt{1+4\pi\xi_0\cot(2\pi\nu)-(2\pi\xi_0)^2}} \tag{A9}$$

The stability criterion for the map requires that $\cos(2\pi(\nu+\Delta\nu))$ should not exceed unity in absolute value. It is easy to see that Eq. (A8) implies that the ranges of values of ξ_0 for which the map is stable are

$$\begin{aligned} \xi_0 &\le \tfrac{1}{2\pi}\cot(\pi\nu) \quad && \text{if } p < \nu < p+\tfrac{1}{2} \\ \xi_0 &\le -\tfrac{1}{2\pi}\tan(\pi\nu) && \text{if } p-\tfrac{1}{2} < \nu < p \end{aligned} \tag{A10}$$

where p is any integer. At the stability limit, corresponding to the equality in the expressions above, the tune shift reaches a finite maximum,

$$\left.\begin{aligned} \Delta\nu_{max} &= p+\tfrac{1}{2}-\nu \quad && \text{if } p < \nu < p+\tfrac{1}{2} \\ \Delta\nu_{max} &= p-\nu && \text{if } p-\tfrac{1}{2} < \nu < p \end{aligned}\right\} \text{ at the stability limit} \tag{A11}$$

One can also look at the stability as a function of ν at fixed ξ_0. From Eqs. (A10) one sees that the possible range of values of the tune is

$$0 < \nu < \frac{1}{\pi}\cot^{-1}(2\pi\xi_0) \tag{A12}$$

with a periodicity of one-half a unit. Thus there is a stopband below every integer and every half-integer,

$$\text{stopbands:} \quad \frac{\mathrm{p}}{2} - \delta\nu < \nu < \frac{\mathrm{p}}{2} \tag{A13}$$

with a stopband width $\delta\nu$ (not to be confused with the tune shift $\Delta\nu$) given by

$$\delta\nu = \frac{1}{2} - \frac{1}{\pi}\cot^{-1}(2\pi\xi_0) = \frac{1}{\pi}\tan^{-1}(2\pi\xi_0) = 2\xi_0 + O\left(\xi_0^3\right) \tag{A14}$$

The dynamical beta function becomes infinitely large at the stability limit. In the simple case of a single kick at the IP, this is explicitly seen in Eq. (A9). This divergence of the beta function is true in the multi-kick case as well: since, by definition, S' vanishes at the stability limit, it follows from Eq. (A6) that β' must diverge unless the (1,2) matrix element of the right-hand side happens to accidentally vanish.

Figures A1 through A4 show the exact numerical solutions of Eqs. (A8) and (A9) for the tune shift and the dynamical beta function, respectively.

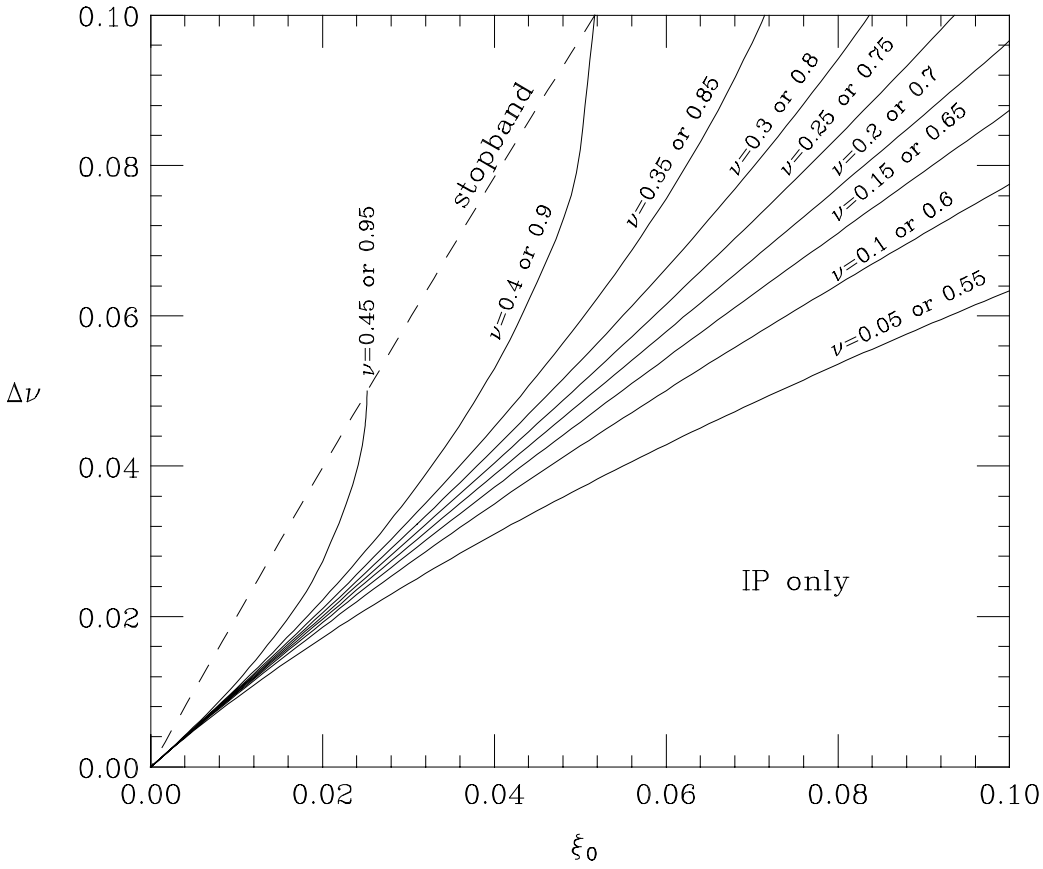

Fig. A1 The beam-beam tune shift produced by a single kick of strength ξ_0 for selected values of ν. For any given tune, $\Delta\nu$ reaches a finite maximum at the stopband, corresponding to ξ_0 given by Eq. (A10).

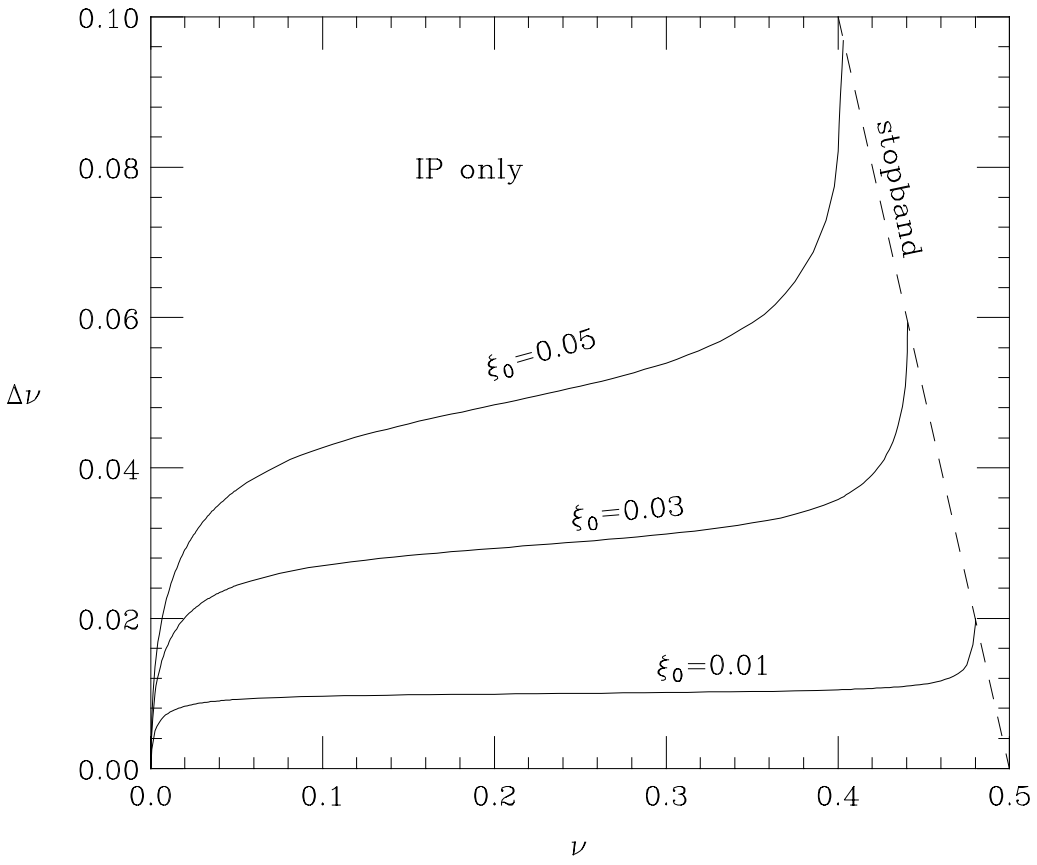

Fig. A2 The beam-beam tune shift produced by a single kick, plotted vs. ν, for selected values of ξ_0. The tune shift reaches a finite maximum at the stopband, corresponding to a tune given by Eq. (A12). The figure is periodic in ν with a period of 0.5.

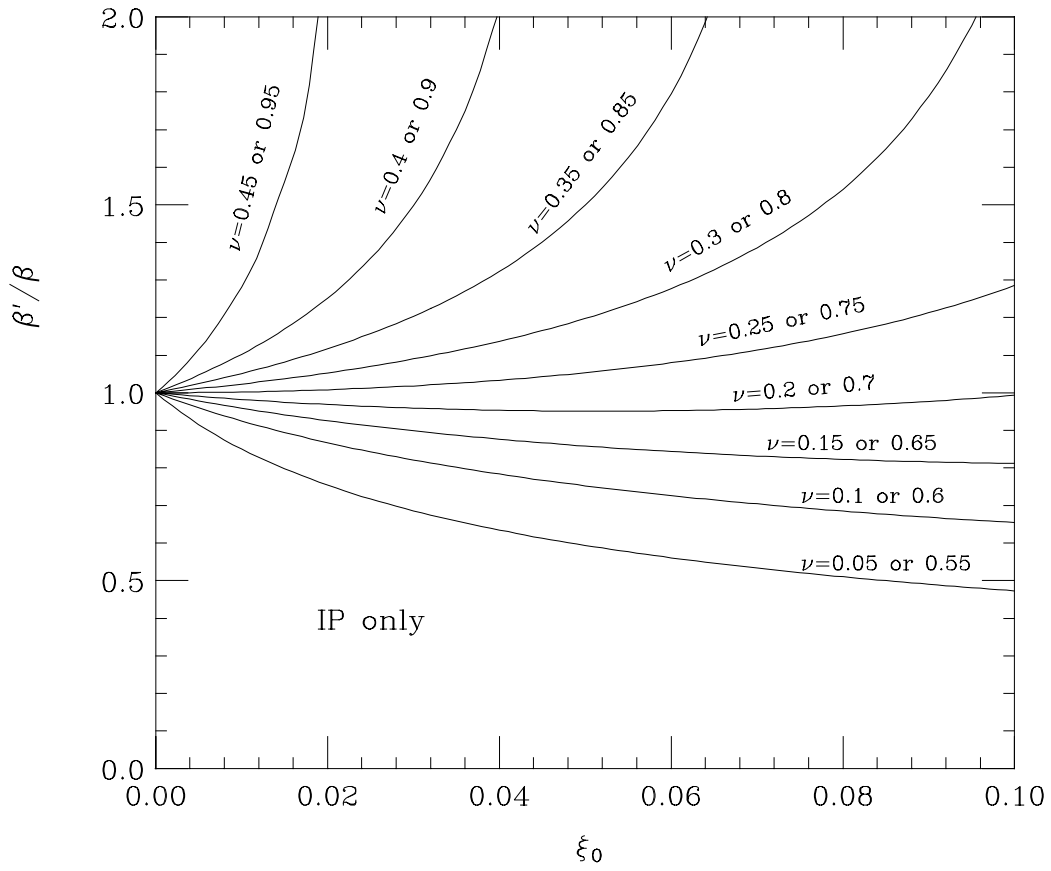

Fig. A3 The normalized dynamical beta function at the IP produced by a single kick of strength ξ_0 for selected values of ν. For any given tune, the dynamical beta function diverges at the stopband, corresponding to a value of ξ_0 given by Eq. (A10).

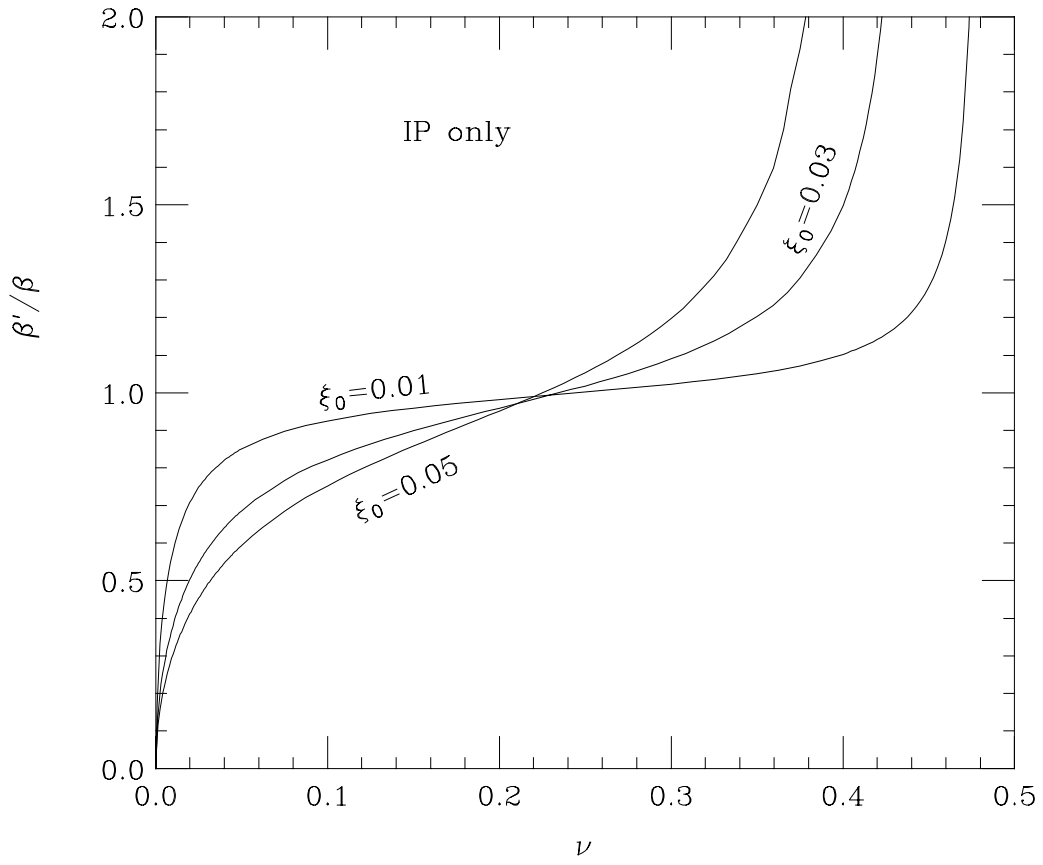

Fig. A4 The normalized dynamical beta function at the IP produced by a single kick, plotted vs. ν, for selected values of ξ_0. The curves become divergent at the stopband, coresponding to a tune given by Eq. (A12). The figure is periodic in ν with a period of 0.5.

A.3 First-order perturbation theory results for the tune shift and the dynamical beta function.

As mentioned earlier, the PCs can have an important effect on the stopband width and location unless they are very weak. For example, in the numerical applications to PEP-II the actual value of the vertical stopband width of the LEB is about 2/3 as large as that computed from the IP alone, as seen in Table 3. The explanation of this relatively large discrepancy is provided by the first-order expression that includes the effects from the PCs, which we now calculate. By writing $\tilde{K}(n)$ in the form

$$\tilde{K}(n) = 1 - 4\pi\xi_n V \ , \qquad \mathrm{V} \equiv \begin{pmatrix} 0 & 0 \\ 1 & 0 \end{pmatrix} \tag{A15}$$

and using the well-known group property of the $\tilde{M}$'s we can expand the product [···] in Eq. (A6) in a power series in the ξ's,

$$\tilde{M}(0,-1)\tilde{K}(-1)\tilde{M}(-1,-2)\cdots\tilde{M}(1,0)\tilde{K}(0)=\tilde{M}(0,0)-4\pi\sum_n \xi_n\tilde{M}(0,n)V\tilde{M}(n,0)+\cdots \qquad \text{(A16)}$$

where $\cdots$ represents higher-order terms in the ξ's, and where $\tilde{M}(0,0)$ is the normalized unperturbed full-turn map,

$$\tilde{M}(0,0)=\begin{pmatrix} C & S \\ -S & C \end{pmatrix}\equiv\begin{pmatrix} \cos(2\pi\nu) & \sin(2\pi\nu) \\ -\sin(2\pi\nu) & \cos(2\pi\nu) \end{pmatrix} \qquad \text{(A17)}$$

The tune shift can be obtained by inserting Eq. (A16) into Eq. (A6) and taking the trace,

$$\begin{aligned} 2C' &= \mathrm{tr}\left\{U(0)^{-1}\left[\tilde{M}(0,-1)\tilde{K}(-1)\tilde{M}(-1,-2)\cdots\tilde{M}(1,0)\tilde{K}(0)\right]U(0)\right\} \\ &= \mathrm{tr}\left[\tilde{M}(0,-1)\tilde{K}(-1)\tilde{M}(-1,-2)\cdots\tilde{M}(1,0)\tilde{K}(0)\right] \\ &= 2C-4\pi S\sum_n \xi_n+\cdots \end{aligned} \qquad \text{(A18)}$$

where we have used $\mathrm{tr}\tilde{M}(0,0)=2C$ and $\mathrm{tr}\left[\tilde{M}(0,n)V\tilde{M}(n,0)\right]=\mathrm{tr}\left[\tilde{M}(0,0)V\right]=S$. Thus the tune shift is given by the familiar equation

$$\cos(2\pi(\nu+\Delta\nu))=\cos(2\pi\nu)-2\pi\sin(2\pi\nu)\sum_n \xi_n+\cdots \qquad \text{(A19)}$$

whose solution, in first-order perturbation theory, is

$$\Delta\nu=\sum_n \xi_n+\cdots \qquad \text{(A20)}$$

The dynamical beta function at the IP is obtained from the (1,2) matrix element in Eq. (A6). Thus we find

$$\beta' S'=\beta S-4\pi\beta\sum_n \xi_n S_{0n}S_{n0}+\cdots \qquad \text{(A21)}$$

where $S_{0n}=\sin(2\pi\nu-\phi_n)$ and $S_{n0}=\sin\phi_n$. Now Eq. (A19) implies, to first order in the ξ's, and assuming that $\sin(2\pi\nu)$ is not too small, that

$$S'=S+2\pi C\sum_n \xi_n+\cdots \qquad \text{(A22)}$$

which, when combined with Eq. (A21), yields the familiar result

$$\frac{\beta'}{\beta}=1-\frac{2\pi}{\sin(2\pi\nu)}\sum_n \xi_n\cos\left(2\Delta\phi_n-2\pi\nu\right)+\cdots \qquad \text{(A23)}$$

In Eqs. (A21) and (A23) the phase advances $\Delta\phi_n$ are relative to the IP, and must be computed by going in the same sense around the ring, e.g., clockwise, as shown in Fig. 1 (thus these $\Delta\phi$'s may depend on the overall tune and are always ≥ 0).

Formula (A23) is a good approximation to the solution of Eq. (A6) provided the tune is not too close to an integer or a half-integer. If this is not the case, the $\sin(2\pi\nu)$ factor in the denominator renders the result invalid. Similarly, formula (A20) for the tune shift is a bad approximation if the tune is close to an integer or a half-integer because $\sin(2\pi\nu)$ appears in the denominator in all higher-order terms. Nevertheless, as in the case of a single kick (cf. Eq. (A11)), the tune shift is actually never divergent.

A.4 First-order perturbation theory results for the stopbands.

Since the phase advances between neighboring PCs are fixed by the optics of the IR, the tune of the ring appears only in the phase advance matrix $\tilde{M}(-4,4)$ for the long arc in Eq. (A6). The form of $\tilde{M}$, Eq. (A5), implies that $\mathrm{tr}M'(0)$ is linear in $\cos(2\pi\nu)$ and $\sin(2\pi\nu)$,

$$\cos(2\pi\nu') = a\cos(2\pi\nu) - b\sin(2\pi\nu) \tag{A24}$$

where a and b depend on the ξ's and on the phases of the collision points but not on the tune. The defining condition for a stopband (i.e., instability) is that $|\cos(2\pi\nu')| \geq 1$. Appropriate use of trigonometric identities implies that the tune is in an interval $\nu_- \leq \nu \leq \nu_+$ where

$$\nu_\pm = \frac{p}{2} - \frac{1}{2\pi}\tan^{-1}\left(\frac{b}{a}\right) \pm \frac{1}{2}\delta\nu \tag{A25}$$

where p is any integer, and where the stopband width $\delta\nu$ is given by

$$\delta\nu = \frac{1}{\pi}\tan^{-1}\sqrt{a^2+b^2-1} \tag{A26}$$

A simple calculation from Eq. (A6) yields the following results, valid for an arbitrary number of beam-beam kicks at arbitrary points in the lattice:

$$\begin{aligned} a &= 1 - \frac{(4\pi)^2}{2}\sum_{n>m}\xi_n\xi_m \sin\Delta\phi_{nm}\sin\Delta\phi_{nm} \\ &\quad + \frac{(4\pi)^3}{2}\sum_{n>m>l}\xi_n\xi_m\xi_l \sin\Delta\phi_{nm}\sin\Delta\phi_{ml}\sin\Delta\phi_{nl} \mp \cdots \\ b &= \frac{4\pi}{2}\sum_n \xi_n - \frac{(4\pi)^2}{2}\sum_{n>m}\xi_n\xi_m \sin\Delta\phi_{nm}\cos\Delta\phi_{nm} \\ &\quad + \frac{(4\pi)^3}{2}\sum_{n>m>l}\xi_n\xi_m\xi_l \sin\Delta\phi_{nm}\sin\Delta\phi_{ml}\cos\Delta\phi_{nl} \mp \cdots \end{aligned} \tag{A27}$$

where the phase advances $\Delta\phi_{nm}$ between kicks *m* and *n* are understood to be computed clockwise along the "short" arc at the top of the ring sketched in Fig. 1. A certain amount of algebra yields

$$a^2 + b^2 - 1 = (2\pi)^2 \left[\sum_n \xi_n^2 + 2 \sum_{n>m} \xi_n \xi_m \cos\left(2\Delta\phi_{nm}\right) \right] + \cdots \tag{A28}$$

where ··· represents terms of higher order in the ξ's.

Now for the case of *symmetrical* IR optics, as in the case of PEP-II, the beam-beam parameters and phases at the PCs satisfy $\xi_n = \xi_{-n}$ and $\phi_n = -\phi_{-n}$. As a result, expression (A28) turns into a perfect square, and (A26) yields

$$\delta\nu = 2\xi_0 + 4\sum_{n\geq 1} \xi_n \cos 2\phi_n + \cdots \tag{A29}$$

for the stopband width, while the edges of the stopband, Eq. (A25), become

$$\begin{aligned} \nu_+ &= \frac{p}{2} - 4\sum_{n\geq 1} \xi_n \sin^2 \phi_n + \cdots \\ \nu_- &= \frac{p}{2} - 2\xi_0 - 4\sum_{n\geq 1} \xi_n \cos^2 \phi_n + \cdots \end{aligned} \tag{A30}$$